**The Plant Cell**
August 2010 ; Vol. 22 (8) : Pages 2825-2837
http://dx.doi.org/10.1105/tpc.109.072215




# The Cytosolic Tail Dipeptide Ile-Met of the Pea Receptor BP80 Is Required for Recycling from the Prevacuole and for Endocytosis[W]

Bruno Saint-Jean[a], Emilie Seveno-Carpentier[b], Carine Alcon[b], Jean-Marc Neuhaus[c] and Nadine Paris[b,*]

[a] Laboratoire de Physiologie et Biotechnologie des Algues, Institut Français de Recherche pour l'Exploitation de la Mer, 44311 Nantes Cedex 03, France
[b] Biochimie et Physiologie Moléculaire des Plantes, Institut de Biologie Intégrative des Plantes, Unité Mixte de Recherche 5004, Centre National de la Recherche Scientifique/Unité Mixte de Recherche 0386, Institut National de la Recherche Agronomique/Montpellier SupAgro/Université Montpellier 2, F-34060 Montpellier Cedex 1, France
[c] Laboratoire de Biologie Moléculaire et Cellulaire, Université de Neuchâtel, CH-2009 Neuchâtel, Switzerland

*: Corresponding author : N. Paris, email address : paris@supagro.inra.fr

**Abstract:**

Pea (*Pisum sativum*) BP80 is a vacuolar sorting receptor for soluble proteins and has a cytosolic domain essential for its intracellular trafficking between the *trans*-Golgi network and the prevacuole. Based on mammalian knowledge, we introduced point mutations in the cytosolic region of the receptor and produced chimeras of green fluorescent protein fused to the transmembrane domain of pea BP80 along with the modified cytosolic tails. By analyzing the subcellular location of these chimera, we found that mutating Glu-604, Asp-616, or Glu-620 had mild effects, whereas mutating the Tyr motif partially redistributed the chimera to the plasma membrane. Replacing both Ile-608 and Met-609 by Ala (IMAA) led to a massive redistribution of fluorescence to the vacuole, indicating that recycling is impaired. When the chimera uses the alternative route, the IMAA mutation led to a massive accumulation at the plasma membrane. Using *Arabidopsis thaliana* plants expressing a fluorescent reporter with the full-length sequence of At VSR4, we demonstrated that the receptor undergoes brefeldin A–sensitive endocytosis. We conclude that the receptors use two pathways, one leading directly to the lytic vacuole and the other going via the plasma membrane, and that the Ileu-608 Met-609 motif has a role in the retrieval step in both pathways.

# 1. Introduction

Pea BP80 (for binding protein of 80 kDa) and its VSR (vacuolar sorting receptor) homologues have been extensively studied these last ten years. BP80 was first identified in clathrin-coated vesicles of developing pea cotyledons by an affinity column using the vacuolar sorting signal from barley proaleurain as bait (Kirsch et al., 1994). Binding occurred at neutral pH (Kd = 37nM) with an optimum at pH6 and was abolished at acidic pH. BP80 was shown to be a type I membrane protein with a single transmembrane domain and a cytosolic C-terminal tail of approximately 5kDa (Kirsch et al., 1994). It was later cloned and characterized and homologues were also identified in Arabidopsis (Paris et al., 1997). In parallel, two homologues were identified AtELP (At3g52850) in Arabidopsis (Ahmed et al., 1997) and PV72 in precursor-accumulating compartments (PAC) from developing pumpkin seeds (Shimada et al., 1997). In Arabidopsis, there are 7 BP80 homologues AtVSR1 to AtVSR7 (Shimada et al., 2003). Except for AtVSR2 (At2g30290) that is expressed only in flowers, the AtVSRs have largely overlapping expression patterns (Laval et al., 1999; Laval et al., 2003; Neuhaus and Paris, 2006). The function of VSRs as a vacuolar sorting receptor was confirmed by several independent studies (Humair et al., 2001; Watanabe et al., 2004; Park et al., 2007). It was also shown that AtVSR1 (AtELP) and PV72 are involved in the calcium-dependent transport of storage proteins (Shimada et al., 1997; Watanabe et al., 2002; Shimada et al., 2003). It was proposed that AtVSR1 serves as a receptor for storage proteins as the *vsr1* knock-out mutant accumulates proforms of globulins and albumins and secretes a large amount of storage proteins (Shimada et al., 2003). Nevertheless, AtVSR1 does not seem to be the vacuolar receptor for aleurain in seeds since *vsr*1 knock-out plants do not miss-sort proaleurain (Shimada et al., 2003). It is still not clear how calcium- and pH-dependent routes interact when the two pathways clearly overlap as in seed cells (Oliviusson et al., 2006; Otegui et al., 2006; Craddock et al., 2008).

Electron microscopy studies showed that VSRs are found in prevacuoles and at the TGN. In pea root tip cells, BP80 was located in the dilated ends of Golgi cisternae. It was also observed in small structures (roughly the size of a vesicle) associated with the outer periphery of 200nm translucent compartments that appear to fuse with the large central vacuole (Paris et al., 1997). In Arabidopsis roots, VSRs were localized to the *trans* face of the Golgi, most likely the TGN and Pep12 compartments (Sanderfoot et al., 1998). VSRs were also found in multivesicular bodies in tobacco BY2 cells (Tse et al., 2004) and in Arabidopsis seeds (Otegui et al., 2006). The receptors mainly concentrates in the prevacuole rather than in the TGN under native conditions (Paris et al., 1997; Li et al., 2002; Tse et al., 2004). VSRs were found mostly in clathrin-coated vesicles (CCVs) (Kirsch et al., 1994; Hohl et al., 1996; Hinz et al., 2007) but could also be detected in dense vesicles containing storage proteins in seeds (Otegui et al., 2006).

Apart from the specialized seed storage compartments, the accepted model of VSR function proposes that VSRs cycle between the TGN and the prevacuole using shuttle vesicles, in particular CCVs (Neuhaus and Paris, 2006). Ligand binding occurs most likely in the lumen of the Golgi or in the TGN. Due to progressive pH acidification along the secretory pathway, as demonstrated in mammalian cells (Perret et al., 2005) and supported by the sensitivity of vacuolar transport to V-ATPase inhibitors (Matsuoka et al., 1997), the receptor releases its ligand in the acidic prevacuole. The free receptor is then recycled back to the TGN by a wortmannin-sensitive mechanism (daSilva et al., 2005) that may involve the retromer complex (Oliviusson et al., 2006). Nevertheless, recent data indicate that the retromer could also play a role at the level of the TGN (Niemes et al., 2010). The released soluble ligands remain in the prevacuolar compartment that most likely matures to a state that is compatible with fusion to the vacuole.

It is believed that multiple cytosolic signals are necessary for receptor trafficking. The tyrosine motif is one of the best studied examples of such signals, particularly in mammals. It is

composed of a tyrosine residue followed by two variable amino acids and a bulky hydrophobic amino acid (YxxΦ). In mammalian cells, the Tyr motifs are involved in clathrin-coated vesicle transport and directly binds to various adaptor proteins depending on their precise sequence (Bonifacino and Traub, 2003, Traub, 2005 #2352). Potential Tyr motifs have been found in plant receptors (Geldner and Robatzek, 2008), but so far have been demonstrated only in BP80 and in the boron transporter BOR1 where it contributes to the recycling mechanism for the polar localization (Takano et al., 2010). The tyrosine motif of AtVSR1 (AtELP), was first shown in vitro by a cross-linking binding assay where a peptide derived from AtVSR1 was able to compete with mammalian sequences containing a tyrosine motif (Sanderfoot et al., 1998). Other in vitro approaches, using pull down assays and surface plasmon resonance measurements, showed that the peaBP80 Tyr motif binds the Arabidopsis μA-adaptin, a Golgi localized protein, with an affinity of 144nM (Happel et al., 2004). Denecke's group studied BP80 trafficking with a nice in vivo competition assay for vacuolar transport (daSilva et al., 2005; daSilva et al., 2006) and found that the tyrosine motif was necessary for Golgi exit. In its absence, the receptor took an alternative route via the plasma membrane. daSilva et al. (2006) showed the two amino acids E604 and I608 to be involved in receptor trafficking. The in vivo confirmation of the role of the motifs in the context of a full-length receptor prompted us to use a similar approach to further investigate the signals of BP80's cytosolic tail and their role in trafficking.
Based on results in the mammalian field (Bonifacino and Traub, 2003; Ghosh et al., 2003), we chose to analyze further (1) the role of acidic amino acids and (2) the role of the IM dipeptide (as part of a dileucine-like motif; EIRAIM). We also further analyzed the role of the tyrosine motif YMPL especially in its relation to other cytosolic signals of BP80.

## 2. Results

Nine different constructs (Figure 1) with selected amino acid substitutions in the cytosolic tail were made from the original PS1 chimera (a GFP linked to the transmembrane and cytosolic domains of pea BP80, Kotzer et al., 2004). We transiently expressed these constructs in tobacco epidermal cells and observed their fluorescence pattern. For PS1, we found punctate fluorescent structures in the cytosol 72 hours after transformation (Figure 2A to 2C). This labeling appeared at the margins in optical sections through the middle of the cell (Figure 2B). In an optical section close to the surface of the cell, spots were easy to visualize (Figure 2B detailed view). One day earlier, 48 hours after transformation, ER labeling was also visible (Figure 2A and inset, ring around the nucleus) and disappeared when the fusion protein had reached its final destination. This labeling is typical for this type of fusion protein and has been extensively described previously (Kotzer et al., 2004; daSilva et al., 2005; daSilva et al., 2006). The spots are mostly prevacuolar compartments and sometimes colocalize with Golgi as expected for the TGN (Figure 2F and Li et al., 2002). To better delineate the distribution of fluorescence we took z-series of the outer half of the cell and stacked the images to make a 3D projection (Figure 2C). We found that in addition to the dominant punctate pattern, fluorescence could also be detected in the plasma membrane (Figure 2B, arrow) and inside the vacuole (Figure 2B, v) but with intensity that slightly varied between cells and expression experiments. We therefore quantified in z stacks the average fluorescence intensity in each of the three subcellular locations: punctate structures, plasma membrane and vacuole (see material and methods for more details). This quantification was made on at least 90 independent measurements for each of the three sub-cellular locations. The average signal intensity obtained for each sub-cellular location was then expressed relative to the total fluorescence (punctate structures plus plasma membrane plus vacuole representing 100%). The quantification shown in Figure 2E for PS1 confirmed that fluorescence is mostly (almost 80%) in dots. To make sure that this distribution reflects final destination of the chimera, we also quantified fluorescence of stably transformed tobacco plants

expressing the PS1 construct (see supplemental Figure S1). Indeed, in these plants the fluorescence was 84% in dots, 14.5% in plasma membrane and 1.5% in vacuole

## Mutations of acidic amino acids have mild effects

We first expressed chimeras with mutations in each of three acidic amino acids found in the cytosolic tail of BP80. Two are conserved in all Arabidopsis homologues (E604 and D616) while the third, E620 is found only in BP80 and its two closest Arabidopsis homologues AtVSR3 and AtVSR4 (At2g14740 and At2g14720). As shown for E604A in a z stack projection (Figure 2D), the labeling pattern for all three mutants was similar to PS1 control. Semi-quantitative intensity measurement confirmed there was no significant difference in distribution, except for a fluorescence increase in the vacuole compared to the control (4 times for D616A and 3 times for E620A, Figure 2E). To find out if these mutations modified protein partitioning between the Golgi/TGN and the prevacuole, we coexpressed each of the three mutants with the Golgi marker ERD2-CFP. As expected, the PS1 construct accumulated mainly in prevacuolar compartments distinct from the Golgi (Figure 2F, arrow). The same was true for the two mutants D616A and E620A (Figure 2H and 2I, respectively). In contrast, the E604A mutant's distribution clearly differed since it colocalized almost exclusively with the Golgi marker (Figure 2G). To conclude, mutating two of the acidic amino acids had mild effects on the reporter's distribution. Mutating E604 increased Golgi localization while mutating D616 and E620 only slightly increased exposition of the fusion protein to a lytic environment.

## Mutation of the tyrosine motif leads to a partial redistribution of the reporter to the plasma membrane

To test the role of the tyrosine motif on the subcellular localization of the reporter, we transiently expressed the mutated chimera Y612A (Figure 1) in tobacco epidermal cells. As shown with a 3D reconstruction of labeled cells, the distribution of the reporter appeared very similar to PS1 except that the plasma membrane seemed more fluorescent than in the control (Figure 3A compared to Figure 2C). To confirm this observation, we performed a quantification of fluorescence intensity in the three subcellular locations punctate structures, plasma membrane and vacuole. There was indeed almost twice as much fluorescence in the plasma membrane compared to the control, with no change in the vacuole (Figure 3C).

## Mutating both I608 and M609 lead to a massive redistribution of the reporter to the vacuole

In order to test the role of the IM dipeptide, we expressed the chimera IMAA where both amino acids were mutated (Figure 1). We analyzed the subcellular localization of the fluorescence after 72 hours of expression. As shown on Figure 3B, the distribution of fluorescence was drastically different from PS1 since the vacuole appeared strongly labeled (Figure 3B, v). The nucleus is visible in negative contrast (Figure 3B, arrow). Quantitatively the IMAA vacuolar fluorescence was found to be 25 times higher than for PS1 (Figure 3C). Fluorescence inside the vacuole can be explained by cleavage and release of the soluble reporter from the membrane-bound fusion protein. We noticed that the vacuolar labeling gradually appeared during the transient expression and peaked at 64h to 72h after transformation. After only 48h of transient expression, fluorescence was found in small dots (Figure 3D and 3E) and then decreased concomitantly with the appearance of vacuolar staining. To gain further insights into the nature of these intermediate compartments, we co-expressed the IMAA construct with the Golgi

reference ERD2-CFP and observed double transformed cells 48 hours after transformation, when spot-type labeling was dominant. As shown in Figure 3F, the compartments labeled with IMAA were almost entirely distinct from the Golgi. We then coexpressed the soluble reporter cargo Aleu-CFP that is transported to the vacuole by VSRs. This reporter contains the vacuolar sorting signal of petunia aleurain that is sufficient for vacuolar targeting (Humair et al., 2001). When expressed in plants, this soluble cargo reporter was also found first in small dots that are believed to be prevacuolar intermediates prior to vacuole delivery (Flückiger et al., 2003, Kotzer, 2004 #1898). When Aleu-CFP was co-expressed with IMAA and cells were observed 48h after transformation, IMAA and Aleu-CFP spots were found to totally colocalize (Figure 3G) indicating the prevacuolar nature of IMAA intermediate compartments. Altogether, this indicates that mutating the IM dipeptide strongly affects the reporter distribution, decreasing Golgi localization in favour of prevacuolar localization. Prevacuolar fluorescence is transient indicating that recycling of the reporter is impaired.

## In contrast to D616 and E620, mutating E604 has some effect even in absence of the tyrosine motif.

We tested the role of the tyrosine motif in relation to the three acidic amino acids by generating double mutants and then transiently expressing them in tobacco epidermal cells. The double mutants had a pattern of expression that resembled the non-mutated control PS1 (data not shown). Quantification revealed that plasma membrane fluorescence intensity for all three mutants was actually closer to Y612A than to PS1 (Figure 4A). In contrast to the single mutants D616A and E620A, fluorescence intensity in the vacuole did not increase for the corresponding double mutants (Figure 4A compared to Figure 2E). This indicates that the tyrosine mutation is dominant and masks the effect of the D616 and E620 mutations. We then addressed the nature of the dots by co-expression with a Golgi reference and found that the E604 mutation caused a redistribution of the marker to the Golgi/TGN (Figure 4C), as already observed with the single mutant (Figure 2G). Since the tyrosine motif mutation is redirecting receptor trafficking to an alternative pathway, this indicates that D616 and E620 are implicated only in the main pathway while E604 is likely to play a role in both pathways.

## Mutating the tyrosine motif showed that the IM dipeptide is also involved in endocytosis

In order to address the relative role of the tyrosine and the IM motifs, we prepared a corresponding double mutant (Figure 1). We transiently expressed the IMAA+Y612A construct in tobacco epidermal cells. The mutant showed a major localization at the plasma membrane with very few intracellular dots (Figure 4F). Quantification of signal intensity clearly confirmed redistribution of this mutant to the plasma membrane (Figure 4I). The signal intensity in the plasma membrane was 3 times higher than than for PS1. To ensure that the whole reporter reached the plasma membrane, we plasmolysed transformed cells. We found that labeling remained associated with the plasma membrane (Figure 4G and 4H, arrow with a star) while the extracellular space was unstained, confirming that the fluorescence was due to the membrane-bound reporter and not to a released and secreted core GFP. The fluorescence intensity at the plasma membrane almost doubled for IMAA+Y612A in comparison to Y612A alone (Figure 4I) indicating that the IMAA motif is important for endocytosis. Additionally, very few spots could also be detected for the IMAA+Y612A reporter. We identified these as being mostly Golgi or closely associated with it since they colocalized with ERD2-GFP (Figure 4J). The fact that we found very little fluorescence in the vacuole for IMAA+Y612A (in contrast to the IMAA mutant)

indicates that the Y612 mutation dominates over the retrieval effect of IMAA maybe by preventing the fusion protein to reach prevacuolar compartments.

## The full length receptor also partially localized to the plasma membrane

To find out if the luminal domain of VSRs could have an influence on the plasma membrane localization of the reporter, we made a fusion protein of the citrine fluorescent protein and the full length receptor. We positioned the fluorescent reporter between the signal peptide and the rest of the sequence of the Arabidopsis homologue AtVSR4 (At2g14720, the closest homologue of pea BP80). This chimera should be functional since a similar construct was able to bind its ligand aleurain in vivo as shown by bimolecular fluorescence complementation (Park et al., 2007). The fusion protein citrine-AtVSR4 was transiently expressed in tobacco epidermal cells and its distribution was observed after 72h of expression. As shown in Figure 5, citrine-AtVSR4 accumulated in dots (Figure 5A) and also in the plasma membrane (Figure 5B) but not in the ER (Figure 5C, n indicates the nucleus). The partitioning of fluorescence between the dots, the plasma membrane and the vacuole was similar to what was found for the PS1 fusion protein. Indeed, the fluorescence intensity in the plasma membrane reached approximately 30% while it represented roughly 20 % without the luminal domain of the receptor. We then addressed the nature of the dots by co-expressing citrine-AtVSR4 with a CFP version of PS1. As shown in Figure 5D, both fusion proteins colocalized. This result indicates that a potentially functional receptor can also be found in the plasma membrane.
We next transformed Arabidopsis plants with the citrine-AtVSR4 chimera. We obtained six fluorescent lines that all presented a dominant spot like labeling as shown in the root apex (Figure 5E). In addition, we observed in all plants an additional plasma membrane labeling. This plasma membrane labeling, was not detectable in root apex cells, but increases gradually along the root's longitudinal axis to be clearly visible in the medium part of the root (Figure 5F) and dominant in the upper part of the root (Figure 5G). In two plants out of six, we could barely detect any dot labeling in cells from the upper region of the root (plant G and H). Since citrine-AtVSR4 is expressed under a 35S promoter, we controlled by immunoblotting the level of protein in comparison to the native receptor. We found similar quantities for the fusion and the native proteins (Figure S2), which indicates that the fluorescent chimera is not massively overexpressed.

## The receptor undergoes endocytic recycling at the plasma membrane.

We took advantage of the exclusive plasma localization of citrine-AtVSR4 in the upper root cells to examine endocytosis and exocytosis. We applied brefeldin A (BFA), a fungal metabolite used to inhibit vesicular trafficking at the exocytosis/secretion level, in presence of the protein biosynthesis inhibitor cycloheximide. In Arabidopsis root cells, BFA treatment leads to the intracellular accumulation of endocytic material in so-called "BFA compartments". Plasma membrane proteins that undergo BFA-sensitive endocytic recycling accumulate in these compartments. Since BFA experiments are usually performed with cells close to the root apex, we performed a control experiment on the upper-root cells expressing the plasma membrane fusion protein LTi6a-GFP (Cutler et al., 2000). As shown on Figure 6B, upper-root cells form typical LTi6a-GFP-containing BFA compartments after BFA treatment as described in apex cells (Dhonukshe et al., 2007). We therefore performed the same treatment on citrine-AtVSR4 expressing roots and found a clear accumulation of fluorescence in BFA bodies (Figure 6A). Interestingly, while an important fraction of LTi6a-GFP remained at the plasma membrane after BFA treatment, we observed a strong decrease to full disappearance of plasma membrane labeling for citrine-AtVSR4 (Figure 6A, arrow). We controlled that labeling of citrine-AtVSR4 was

stable along the duration of the experiment by treatment with cycloheximide alone (Figure 6C) or DMSO (not shown). The accumulation of citrine-AtVSR4 in BFA compartment together with a decrease of plasma membrane labeling indicates that the receptor undergoes endocytosis. In contrast to the LTi6a-GFP control, we also observed a faster accumulation of citrine-AtVSR4 in BFA compartments (10 min of BFA treatment compared to 60 min for Lti6a-GFP). We next tested the ability of the receptor to participate in exocytosis by washing off the BFA in presence of cycloheximide. As shown on Figure 6D and 6E, BFA compartments visible before washing (Figure 6D) disappeared after removal of BFA while plasma membrane labeling was recovered (Figure 6E). This indicates that the receptor can traffic from internal compartments to the plasma membrane. In conclusion, plasma membrane localized citrine-AtVSR4 undergoes BFA-sensitive exo- and endocytic cycling.

## 3. Discussion

### *VSR trafficking and signals*

The main result of this study is the identification and characterization of a novel signal, the dipeptide IM that is conserved in all the VSRs identified so far. IM is involved in two trafficking steps: (1) the recycling from the PVC and (2) endocytosis. Based on our results, and on previous observations of daSilva (daSilva et al., 2006), we propose the following model (Figure 7) with a main pathway (double arrows) and an alternative pathway (simple arrows). In the main pathway, the receptor recognizes its ligand in the TGN, releases it into the prevacuole and recycles back to the TGN. The contention that acidification is a necessary component for vacuolar transport is supported (1) by *in situ* pH measurements in mammalian cells giving values of 6.2 in the TGN and less than 5,5 in the prelysosomal compartment (Anderson and Orci, 1988; Miesenböck et al., 1998), (2) by the fact that V-ATPase inhibitors disrupts the transport of vacuolar soluble cargo in plants (Matsuoka et al., 1997) and (3) by pH-dependent binding of VSR to its ligands (Kirsch et al., 1994). As previously suggested (daSilva et al., 2006), we found that the tyrosine motif is used for the exit step from the TGN to the PVC/MVB (Figure 7, step 1). The observed vacuolar accumulation increase of released core GFP argues for a major role of IM and for a minor role of D616 and D620 in the retrieval step (Figure 7, step 3). The requirement of the cytosolic domain and in particular of a functional tyrosine motif to efficiently reach the post-Golgi lytic compartments is also supported by the Golgi accumulation of a fusion protein lacking the whole cytosolic domain of VSR (Brandizzi et al., 2002).

The alternative pathway involves the TGN/early endosome and the plasma membrane (simple arrows, Figure 7). In the absence of a functional tyrosine motif, the receptor is forced to take this alternative route as indicated by an increase of plasma membrane labeling. The remaining presence of internal labeling when the Y612A construct was used indicates either that the transport from the TGN to plasma membrane is not very efficient or that internalization of the receptor counterbalances the effect of mutating the tyrosine. We found that mutating the IM dipeptide in addition to the tyrosine doubles the fluorescence intensity at the plasma membrane, inverting the proportions of dots and plasma membrane in comparison to a non-mutated receptor. This clearly indicates that IM is involved in this endocytosis step. We cannot exclude the possibility that the tyrosine motif functions as well in endocytosis since Y612A is also partially accumulated in the plasma membrane. Surprisingly, we found no increase of vacuolar labeling when mutating IMAA and Y612A together. We therefore propose that the alternative pathway does not include compartments that reside further down the early endosome on the vacuole route. Instead, we propose that the Y612A mutant cycles between the plasma membrane and the early endosome (EE). We confirmed that the receptor undergoes a BFA-sensitive endocytic cycling in Arabidopsis transgenic plants expressing a fusion protein with the

entire sequence of AtVSR4 at a level similar to the endogenous form. Plant apoplastic environment is compatible with ligand recognition since optimal pH for VSR binding is approximately 6.2 (Kirsch et al., 1994) and averaged extracellular pH is 6 (Grignon and Sentenac, 1991; Gao et al., 2004). Therefore, the plasma membrane-EE pathway identified in our expression and mutation assays is not a default pathway due to overexpression, but an alternative pathway taken actively by the receptor, most likey to retrieve ligands that escaped the sorting step at the TGN, like the mammalian mannose-6-phosphate receptors (MPR) do for escaped lysosomal proteins (Ghosh et al., 2003). The fact that VSRs were isolated from a purified plasma membrane fraction also supports this conclusion (Laval et al., 1999).
Two publications show that the TGN, labeled by the secretory carrier membrane protein 1 (SCAMP1) and the v-ATPase subunit VHA1, is the first intracellular station of endocytosed cargoes before going to multivesicular bodies (MVB) (Dettmer et al., 2006; Lam et al., 2007). These two publications indicate that in plants the TGN, defined by electron microscopy as a Golgi-associated partially clathrin-coated reticulum (PCR), may also function of an early endosome (EE). It is likely that the EE and the TGN may represent subdomains of a same PCR compartment. The receptor could move from EE to the TGN and use either one of the two pathways (Figure 7, step 10).
We also addressed the role of acidic residues in the cytosolic tail and found that their mutations had minor effects on VSR trafficking. E604 may participate either in some early transport step prior to the splitting point between the two pathways, while D616 and D620 may participate in recycling from the prevacuole. This is in accordance with daSilva's results (daSilva et al., 2006) where E604A caused a strong loss in the competitive effect of the mutated receptor, without changing core-GFP release.

### *VSR trafficking partners*

VSRs are so far the only examples of plant receptors with a demonstrated trafficking signal using clathrin coated vesicles. The mechanism of clathrin coat assembly at Golgi and plasma membrane is well described in mammalian cells (Traub, 2005). The coat is composed of an inner layer of adaptors and an outer layer of clathrin. Adaptors play a key role by interacting with both the membrane cargo (or receptors) and the clathrin. Cargo incorporation into the complex is highly regulated with the implication of 4 classes of signals carried by the cargo or the receptors: the tyrosine motif (YxxØ), the acidic cluster-dileucine signal (DxxLL), the dileucine signal ([D/E]xxxL[L/I/M]) and the tyrosine-based motif (FxNPxY). The µ subunits of adaptor complexes bind to the tyrosine motif with preferences of each type of µ protein (1 to 4) being mainly determined by residues in positions 2, 3 and 4 of the Tyr motif (Ohno et al., 1998; Bonifacino and Traub, 2003). All plant VSRs identified so far contain a conserved tyrosine motif (YMPL). The Arabidopsis µA-adaptin, part of the AP2 subclass, could bind to the tyrosine motif of VSRs at the level of the TGN (Ahmed et al., 2000; Happel et al., 2004).

### *Endocytosis and a putative dileucine motif*

Endocytosis was long considered impossible in plants because turgor pressure would prevent membrane invagination. It is now clear from numerous independent studies that endocytosis can occur, even in guard cells. With the help of fluorescent proteins and drugs such as wortmannin and BFA, our knowledge of endosomal compartments has greatly progressed as reviewed recently (Geldner and Robatzek, 2008; Robinson et al., 2008). In plants, a role of a tyrosine motif in endocytosis is supported by the fact the human transferrin receptor appears to be functional for endocytosis in plant cells (Ortiz-Zapater et al., 2006). Very recently a Tyr motif was found to be implicated in the endocytosis-mediated polar localization of Arabidopsis BOR1

(Takano et al., 2010). When cryptogein, a molecule derived from an oomycete, was applied to BY2 tobacco cells, it enhanced the uptake of the lipophilic reagent FM4-64, a classical marker for endocytosis. The number of clathrin-coated pits was also found to increase upon cryptogein treatment and tyrphostin A23 had antagonistic effect on cryptogein-induced endocytosis (Leborgne-Castel et al., 2008).
In the case of VSRs, tyrosine 612 has been shown to be part of a tyrosine motif and its binding to a Golgi localized μA adaptin supports a function in the TGN exit step (Happel et al., 2004). This nevertheless does not exclude a function in endocytosis where the dipetide IM clearly plays a role. The context of IM dipeptide, ExxxIM, resembles to the canonic sequence of a dileucine signal [D/E]xxxL[L/I/M]. In mammalian cells, such signals have been identified as endocytosis signals in several membrane proteins including CD3 γ-chain and mannose 6-phosphate receptors. This motif binds to the μ subunit of AP1, 2 and 3. The ExxxIM in VSRs could be such an endocytic dileucine-like motif. In mammalian cells, the acidic residue appears to be important for targeting to later endosomal compartments but not for the internalization itself (Pond et al., 1995; Sandoval et al., 2000). This fits with our observation that the E604 mutation did not affect endocytosis in the Y612A mutant.

### *The IM motif contributes to two pathways*

The IM motif found in VSRs clearly plays a dual role in receptor trafficking. There is at least one example of a similar motif in a mammalian receptor that also plays a dual role in trafficking. Like VSRs, the cation-independent mannose-6-phosphate receptor (CI-MPR) is involved in transporting lytic enzymes and is present in the TGN, the early endosomes, the recycling endosomes and in the plasma membrane (Ghosh et al., 2003). Its cytosolic domain contains numerous trafficking signals including a tyrosine motif (YSKV) and the tripeptide WLM which has a dual function. Having identified the latter by an alanine scan on a portion of CI-MPR, Seaman found that its mutation lead to a massive degradation of the reporter fusion protein CD8-CI-MPR, therefore demonstrating its role in recycling. This tripeptide is also required for binding to retromer proteins VPS26 and VPS29. These features are shared with a similar tripeptide FLV in sortilin leading to the conclusion that [W/F]L[M/V] is a consensus motif for retromer-mediated retrieval from endosomes to TGN in mammals (Seaman, 2007). Interestingly, WLM in CI-MPR is also part of a dileucine motif ETEWLM that binds the γ and σ subunits from the adaptator complex AP1 (Traub, 2005) but also favors binding of the tyrosine motif to the μ subunit of the same AP1 complex (Lee et al., 2008). In support of these results, Seaman found that neither AP1 nor retromer could be co-immunoprecipitated with CI-MPR when WLM was mutated but he also demonstrated that the retromer and the AP1 complexes mediate two distinct pathways. Therefore, the tripeptide WLM of CI-MPR is both a retrieval signal for the retromer and a dileucine-like signal for the AP1-mediated transport in cooperation with the tyrosine motif. In VSRs, the IM could correspond to the retromer association signal [W/F]L[M/V], although the preceding amino acid is never aromatic in any VSR identified so far but is instead almost always an Ala and rarely a Ser or a Thr.
In our model the same IM motif is used in two different trafficking steps of VSR trafficking but in the main pathway the receptor is ligand-free while it would be bound in the alternative route. In some mammalian receptors, dileucine signals are modulated by serine phosphorylation (Pitcher et al., 1999; von Essen et al., 2002). Interestingly, the dileucine-like signal of VSRs is also preceded by a serine (SExxxIM) which is predicted to have a good probability of in vitro phosphorylation (Blom et al., 1999).

# 4. Methods

## Constructs

The coding sequence for GFP-PS1 was described previously (Kotzer et al., 2004) and contains the green fluorescent protein (GFP) reporter followed by the transmembrane and the cytosolic domains of pea BP80 (Paris et al., 1997)). We used the described previously GFP6 (Di Sansebastiano et al., 2001), with the double mutation F64L and S65T (Cormack et al., 1996).
A Sal1 site was created at the fusion between the GFP and BP80 with no change in either one of the two sequences and a Sac1 site was added at the level of the stop codon. The resulting coding sequence at the fusion is MDELYKSTW*AAF* where the underlined K, preceding the transmembrane domain (italic), is shared by GFP and BP80 sequences. Point mutations, changing chosen amino acids to alanine, were introduced in the cytosolic sequence of BP80 by overlapping PCR. The resulting PCR fragment was controlled by sequencing and used to substitute the original sequence using Sal1 and Sac1 sites. This generated 9 new constructs named according to the point mutations introduced at the level of the cytosolic domain of pea BP80; E604A, IMAA, YA, D616A, E620A, E604AYA, IMAAYA YAD616A and YAE620A. For easier comparison with published data (daSilva et al., 2006), these numbers correspond to the positions of targeted amino acids in reference to the sequence of the Arabidopsis homologue AtVSR3. All constructs were finally transferred into the binary vector pVKH18En6 for transient expression under the control of the strong 35S promoter (Batoko et al., 2000).
Fusing citrine sequence (Griesbeck et al., 2001) with the full length of AtVSR4 (At2g14720) was made by inserting the reporter between the signal peptide and the sequence of the mature AtVSR4 by creating a Pst1 in 5' and a Spe1 in 3' junctions. The resulting fusion was cloned into the Gateway vector pK2GW7 under the control of a 35S promoter.
The ERD2-CFP construct was previously described in Chatre et al (Chatre et al., 2005). Aleu-GFP was previously described (Humair et al., 2001) and a CFP version was made by replacing the GFP6 with an eCFP sequence. The resulting aleu-CFP carries the signal peptide of tobacco chitinase and the vacuolar sorting propeptide from *Petunia hybrida* aleurain (RTANFADENPIRQVVSDSFHELES) fused to the sequence of the reporter.

## Expression in plants and confocal microscopy

For transient expression in tobacco leaves, 3 to 4 weeks old *Nicotiana tabacum* cv SR1 plants were used. The construct carried by the binary vector was introduced into plant cells *via* infiltration of a transformed *Agrobacterium tumefaciens* strain GV3101 p2260 as described previously (Brandizzi et al., 2002). The agrobacteria suspension was inoculated at a density of $OD_{600}$ = 0.3 in the lower epidermis after making a small lesion to facilitate the infiltration. We kept the plants in the dark during expression to allow optimal visualization of vacuolar labeling. We observed the fluorescence 24 to 72hr after transient expression in tobacco epidermal cells from a small leaf piece cut off the plant and mounted in water between slide and coverslip.
Arabidopsis thaliana (ecotype columbia) was transformed with the "floral dip" method (Clough and Bent, 1998) using the *Agrobacterium tumefaciens* strain GV3101 p2260.

We used either a Leica TCS sp2 (Platform for Cell Imaging of Haute-Normandie PRIMACEN) or an inverse 1 axiovert 200M Zeiss/LSM 510 META confocal microscope (Montpellier RIO imaging platform). For imaging of the co-expression of CFP and GFP6, we used a sequential mode with the 458 and 488nm laser excitation lines from this microscope. In more details, the 458nm and 488nm lines were alternatively switched on to detect respectively the CFP fluorescence (from 460nm to 485nm) and the GFP6 fluorescence (from 509nm to 602nm). The laser power was set

to the minimum required for a sharp but not saturating signal and appropriate controls were made to ensure there was no bleed-through from one channel to the other. That is, we ensured that the signal collected for one fluorochrome remains unchanged when the laser line used to excite the second fluorochrome was switched off. Images were mounted using Adobe Photoshop 7.0 software (Mountain View, CA).

## Quantification of fluorescent signal

Fluorescence was analyzed using the software provided with the confocal microscope (Leica confocal software 2.5). We aimed to obtain quantitative data on the distribution of fluorescence in three main subcellular locations named punctate structures, plasma membrane and vacuole. Prior to quantification, we controlled that the fusion protein had reached its final destination by the absence of ER labeling in a confocal section through the nucleus. We first acquired z-series of transformed cells, with 1µm z-step. Laser power was set manually for each single cell at the most fluorescent section to get the maximum signal but just below the saturation level. This setting ensures that the fluorescence signal is optimal but linear and comparable within different sections of a given cell. Regions of interest (ROIs) were then drawn manually at different locations and in different sections of the z-series. ROI were drawn to contain only fluorescent signal from the subcellular location chosen; punctate structure, plasma membrane or vacuole content. The mean intensity of fluorescence was measured for each ROI. This measurement was repeated at least 5 times for one cell, within different z-sections. We repeated measurements on 6 to 10 z-series coming from 3 independent transient expressions. The relative distribution of signal within spots, vacuole and plasma membrane was then expressed setting arbitrarily 100% as being the sum of the three types of intensity measured.

## Plant culture and drug treatments

Arabidospis thaliana plants (columbia) expressing Pro35S:citrine-AtVSR4 (this study) or LTi6a-GFP (Cutler et al., 2000) were grown on plate with MS/2 medium for a week. Drugs were applied by transferring one-week old plantlets from the plate on a drop of diluted chemicals. Brefeldin A (Sigma) and cycloheximide (Sigma) were both used at a concentration of 50µM for times indicated in the result section (10 to 60 minutes). Dilution was made freshly from a 1000x stock solution in DMSO.

## Supplemental data

Supplemental figure 1 : Expression of PS1 fusion protein in tobacco plants.
Supplemental figure 2 : Arabidopsis expressing stably the construct citrine-AtVSR4 produce the fusion protein in a similar amount than the native homologue.

## References


**Ahmed, S.U., Bar-Peled, M., and Raikhel, N.V.** (1997). Cloning and subcellular location of an Arabidopsis receptor-like protein that shares common features with protein-sorting receptors of eukaryotic cells. Plant Physiology **114:** 325-336.

**Ahmed, S.U., Rojo, E., Kovaleva, V., Venkataraman, S., Dombrowski, J.E., Matsuoka, K., and Raikhel, N.V.** (2000). The plant vacuolar sorting receptor AtELP is involved in transport of $NH_2$-terminal propeptide-containing vacuolar proteins in *Arabidopsis thaliana.* Journal of Cell Biology **149:** 1335-1344.

**Anderson, R., and Orci, L.** (1988). A view of acidic intracellular compartments. Journal of Cell Biology **106:** 539-543.

**Batoko, H., Zheng, H.-Q., Hawes, C., and Moore, I.** (2000). A Rab1 GTPase is required for transport between endoplasmic reticulum and Golgi apparatus and for normal Golgi movement in plants. Plant Cell **12:** 2201-2217.

**Blom, N., Gammeltoft, S., and Brunak, S.** (1999). Sequence- and structure-based prediction of eukaryotic protein phosphorylation sites. Journal of Molecular Biology **294:** 1351-1362.

**Bonifacino, J., and Traub, L.** (2003). Signals for sorting of transmembrane proteins to endosomes and lysosomes. Annu Rev Biochem. **72:** 395-447.

**Brandizzi, F., Frangne, N., Marc-Martin, S., Hawes, C., Neuhaus, J.-M., and Paris, N.** (2002). In plants the destination for single pass membrane proteins is markedly influenced by the length of the hydrophobic domain. Plant Cell **14:** 1077-1092.

**Chatre, L., Brandizzi, F., Hocquellet, A., Hawes, C., and Moreau, P.** (2005). Sec22 and Memb11 are v-SNAREs of the anterograde endoplasmic reticulum-Golgi pathway in tobacco leaf epidermal cells. Plant Physiology **139:** 1244-1254.

**Clough, S.J., and Bent, A.F.** (1998). Floral dip: a simplified method for Agrobacterium-mediated transformation of Arabidopsis thaliana. Plant Journal **16:** 735-743.

**Cormack, B.P., Valdivia, R.H., and Falkow, S.** (1996). FACS-optimized mutants of the green fluorescent protein (gfp). Gene **173:** 33-38.

**Craddock, C., Hunter, P., Szakacs, E., Hinz, G., Robinson, D., and Frigerio, L.** (2008). Lack of a vacuolar sorting receptor leads to non-specific missorting of soluble vacuolar proteins in Arabidopsis seeds. Traffic **9:** 408-416.

**Cutler, S.R., Ehrhardt, D.W., Griffitts, J.S., and Somerville, C.R.** (2000). Random GFP :: cDNA fusions enable visualization of subcellular structures in cells of Arabidopsis at a high frequency. Proceedings of the National Academy of Sciences of the United States of America **97:** 3718-3723.

**daSilva, L., Foresti, O., and Denecke, J.** (2006). Targeting of the plant vacuolar sorting receptor BP80 is dependent on multiple sorting signals in the cytosolic tail. The Plant Cell **18:** 1477-1497.

**daSilva, L.L., Taylor, J.P., Hadlington, J.L., Hanton, S.L., Snowden, C.J., Fox, S.J., Foresti, O., Brandizzi, F., and Denecke, J.** (2005). Receptor salvage from the prevacuolar compartment is essential for efficient vacuolar protein targeting. The Plant Cell **17:** 132-148.

**Dettmer, J., Hong-Hermesdorf, A., Stierhof, Y.-D., and Schumacher, K.** (2006). Vacuolar $H^+$-ATPase activity is required for endocytic and secretory trafficking in Arabidopsis. The Plant Cell **18:** 715-730.

**Dhonukshe, P., Aniento, F., Hwang, I., Robinson, D., Mravec, J., Stierhof, Y., and Friml, J.** (2007). Clathrin-mediated constitutive endocytosis of PIN auxin efflux carriers in Arabidopsis. Current Biology **17:** 520-527.

**Di Sansebastiano, G.-P., Paris, N., Marc-Martin, S., and Neuhaus, J.-M.** (2001). Regeneration of a lytic central vacuole and of neutral peripheral vacuoles can be visualised by GFP targeted to either type of vacuoles. Plant Physiol. **126:** 78-86.

**Flückiger, R., De Caroli, M., Piro, G., Dalessandro, G., Neuhaus, J.-M., and Di Sansebastiano, G.-P.** (2003). Vacuolar system distribution in *Arabidopsis* tissues, visualized using GFP fusion proteins. Journal of Experimental Botany **54:** 1577-1584.
**Gao, D., Knight, M., Trewavas, A., Sattelmacher, B., and Plieth, C.** (2004). Self-reporting Arabidopsis expressing pH and [Ca2+] indicators unveil ion dynamics in the cytoplasm and in the apoplast under abiotic stress. Plant Physiology **134:** 898-908.
**Geldner, N., and Robatzek, S.** (2008). Plant receptors go endosomal: A moving view on signal transduction. Plant Physiol. **147:** 1565-1574.
**Ghosh, P., Dahms, N., and Kornfeld, S.** (2003). Mannose 6-phosphate receptors: new twists in the tale. Nature Reviews of Molecular Cell Biology **4:** 202-213.
**Griesbeck, O., Baird, G.S., Campbell, R.E., Zacharias, D.A., and Tsien, R.Y.** (2001). Reducing the environmental sensitivity of yellow fluorescent protein. Journal of Biological Chemistry **276:** 29188-29194.
**Grignon, C., and Sentenac, H.** (1991). pH and ionic conditions in the apoplast. Annual Review of Plant Physiology and Plant Molecular Biology **42:** 103-128.
**Happel, N., Höning, S., Neuhaus, J.-M., Paris, N., Robinson, D.G., and Holstein, S.E.H.** (2004). Arabidopsis µA-adaptin interacts with the tyrosine motif of the vacuolar sorting receptor VSR-PS1. Plant Journal **37:** 678-693.
**Hinz, G., Colanesi, S., Hillmer, S., Rogers, J., and Robinson, D.** (2007). Localization of vacuolar transport receptors and cargo proteins in the Golgi apparatus of developing Arabidopsis embryos. Traffic **8:** 1452–1464.
**Hohl, I., Robinson, D.G., Chrispeels, M.J., and Hinz, G.** (1996). Transport of storage proteins to the vacuole is mediated by vesicles without a clathrin coat. J. Cell Sci. **109:** 2539-2550.
**Humair, D., Hernández Felipe, D., Neuhaus, J.-M., and Paris, N.** (2001). Demonstration in yeast of the function of BP-80, a putative plant vacuolar sorting receptor. The Plant Cell **13:** 781-792.
**Kirsch, T., Paris, N., Butler, J.M., Beevers, L., and Rogers, J.C.** (1994). Purification and initial characterization of a potential plant vacuolar targeting receptor. Proc. Natl. Acad. Sci. USA **91:** 3403-3407.
**Kotzer, A.M., Brandizzi, F., Neumann, U., Paris, N., Moore, I., and Hawes, C.** (2004). *At*RabF2b (Ara7) acts on the vacuolar trafficking pathway in tobacco epidermal cells. Journal of Cell Science **117:** 6377-6389.
**Lam, S., Siu, C., Hillmer, S., Jang, S., An, G., Robinson, D., and Jiang, L.** (2007). Rice SCAMP1 defines clathrin-coated, trans-Golgi–located tubular-vesicular structures as an early endosome in Tobacco BY-2 cells. Plant Cell **19:** 296-319.
**Laval, V., Chabannes, M., Carrière, M., Canut, H., Barre, A., Rougé, P., Pont-Lezica, R., and Galaud, J.-P.** (1999). A family of *Arabidopsis* plasma membrane receptors presenting animal ß-integrin domains. Biochim. Biophys. Acta **1435:** 61-70.
**Laval, V., Masclaux, F., Serin, A., Carrière, M., Roldan, C., Devic, M., Pont-Lezica, R.F., and Galaud, J.-P.** (2003). Seed germination is blocked in *Arabidopsis* putative (atbp80) antisense transformants. Journal of Experimental Botany **54:** 213-221.
**Leborgne-Castel, N., Lherminier, J., Der, C., Fromentin, J., Houot, V., and Simon-Plas, F.** (2008). The plant defense elicitor cryptogein stimulates clathrin-mediated endocytosis correlated with reactive oxygen species production in bright yellow-2 Tobacco cells. Plant Physiol. **146:** 1255-1266.
**Lee, I., Doray, B., Govero, J., and Kornfeld, S.** (2008). Binding of cargo sorting signals to AP-1 enhances its association with ADP ribosylation factor 1–GTP. Journal of Cell Biology **180:** 467-472.
**Li, Y.-B., Rogers, S.W., Tse, Y.C., Lo, S.W., Sun, S.S.M., Jauh, G.-Y., and Jiang, L.** (2002). BP-80 and homologs are concentrated on post-Golgi, probable lytic prevacuolar compartments. Plant & Cell Physiology **43:** 726-742.

**Matsuoka, K., Higuchi, T., Maeshima, M., and Nakamura, K.** (1997). A vacuolar-type $H^+$-ATPase in a nonvacuolar organelle is required for the sorting of soluble vacuolar protein precursors in tobacco cells. Plant Cell **9:** 533-546.
**Miesenböck, G., De Angelis, D., and Rothman, J.** (1998). Visualizing secretion and synaptic transmission with pH-sensitive green fluorescent proteins. Nature **394:** 192-195.
**Neuhaus, J.-M., and Paris, N.** (2006). Plant Vacuoles: from biogenesis to function. In Plant Endocytosis, J. Samaj, F. Baluska, and D. Menzel, eds (Berlin Heidelberg: Springer-Verlag), pp. 63-82.
**Niemes, S., Langhans, M., Viotti, C., Scheuring, D., Yan, M., Jiang, L., Hillmer, H., Robinson, D., and Pimpl, P.** (2010). Retromer recycles vacuolar sorting receptors from the trans-Golgi network. Plant Journal **61:** 107-121.
**Ohno, H., Aguilar, R.C., Yeh, D., Taura, D., Saito, T., and Bonifacino, J.S.** (1998). The medium subunits of adaptor complexes recognize distinct but overlapping sets of tyrosine-based sorting signals. J. Biol. Chem. **273:** 25915-25921.
**Oliviusson, P., Heinzerling, O., Hillmer, S., Hinz, G., Tse, Y.C., Jiang, L., and Robinson, D.G.** (2006). Plant retromer, localized to the prevacuolar compartment and microvesicles in Arabidopsis, may interact with vacuolar sorting receptors. Plant Cell **18:** 1239-1252.
**Ortiz-Zapater, E., Soriano-Ortega, E., Jesús Marcote, M., Ortiz-Masiá, D., and Aniento, F.** (2006). Trafficking of the human transferrin receptor in plant cells: effects of tyrphostin A23 and brefeldin A. The Plant Journal **48:** 757–770.
**Otegui, M., Herder, R., Schulze, J., Jung, R., and Staehelin, L.** (2006). The proteolytic processing of seed storage proteins in Arabidopsis embryo cells starts in the multivesicular bodies. Plant Cell **18:** 2567-2581.
**Paris, N., Rogers, S.W., Jiang, L., Kirsch, T., Beevers, L., Phillips, T.E., and Rogers, J.C.** (1997). Molecular cloning and further characterization of a probable plant vacuolar sorting receptor. Plant Physiology **115:** 29-39.
**Park, J., Oufattole, M., and Rogers, J.** (2007). Golgi-mediated vacuolar sorting in plant cells: RMR proteins are sorting receptors for the protein aggregation/membrane internalization pathway. Plant Science **172:** 728-745.
**Perret, E., Lakkaraju, A., Deborde, S., Schreiner, R., and Rodriguez-Boulan, E.** (2005). Evolving endosomes: how many varieties and why? Curr Opin Cell Biol **17:** 423-434.
**Pitcher, C., Honing, S., Fingerhut, A., Bowers, K., and Marsh, M.** (1999). Cluster of differentiation antigen 4 (CD4) endocytosis and adaptor complex binding require activation of the CD4 endocytosis signal by serine phosphorylation. Mol Biol Cell. **10:** 677-691.
**Pond, L., Kuhn, L., Teyton, L., Schutze, M.-P., Tainer, J., Jackson, M., and Peterson, P.** (1995). A role for acidic residues in di-leucine motif-based targeting to the endocytic pathway. J. Biol. Chem. **270:** 19989-19997.
**Robinson, D., Jiang, L., and Schumacher, K.** (2008). The endosomal system of plants: charting new and familiar territories. Plant Physiol. **147:** 1482-1492.
**Sanderfoot, A.A., Ahmed, S.U., Marty-Mazars, D., Rapoport, I., Kirchhausen, T., Marty, F., and Raikhel, N.V.** (1998). A putative vacuolar cargo receptor partially colocalizes with atPEP12p on a prevacuolar compartment in *Arabidopsis* roots. Proc. Natl. Acad. Sci USA **95:** 9920-9925.
**Sandoval, I., Martinez-Arca, S., Valdueza, J., Palacios, S., and Holman, G.** (2000). Distinct reading of different structural determinants modulates the dileucine-mediated transport steps of the lysosomal membrane protein LIMPII and the insulin-sensitive glucose transporter GLUT4. J. Biol. Chem. **275:** 39874-39885.
**Seaman, M.N.J.** (2007). Identification of a novel conserved sorting motif required for retromer-mediated endosome-to-TGN retrieval. J Cell Sci **120:** 2378-2389.

**Shimada, T., Kuroyanagi, M., Nishimura, M., and Hara-Nishimura, I.** (1997). A pumpkin 72-kDa membrane protein of precursor-accumulating vesicles has characteristics of a vacuolar sorting receptor. Plant & Cell Physiology **38:** 1414-1420.
**Shimada, T., Fuji, K., Tamura, K., Kondo, M., Nishimura, M., and Hara-Nishimura, I.** (2003). Vacuolar sorting receptor for seed storage proteins in *Arabidopsis thaliana*. Proc. Natl. Acad. Sci USA **100:** 16095-16100.
**Takano, J., Tanaka, M., Toyoda, A., Miwa, K., Kasai, K., Fuji, K., Onouchi, H., Naito, S., and Fujiwara, T.** (2010). Polar localization and degradation of Arabidopsis boron transporters through distinct trafficking pathways. Proc Natl Acad Sci U S A **107:** 5220-5225.
**Traub, L.** (2005). Common principles in clathrin-mediated sorting at the Golgi and the plasma membrane. Biochimica et Biophysica Acta (BBA) - Molecular Cell Research **1744:** 415-437.
**Tse, Y.C., Mo, B., Hillmer, S., Zhao, M., Lo, S.W., Robinson, D.G., and Jiang, L.** (2004). Identification of multivesicular bodies as prevacuolar compartments in *Nicotiana tabacum* BY2 cells. The Plant Cell **16:** 672-693.
**von Essen, M., Menné, C., Nielsen, B., Lauritsen, J., Dietrich, J., Andersen, P., Karjalainen, K., Ødum, N., and Geisler, C.** (2002). The CD3 $\gamma$ leucine-based receptor-sorting motif is required for efficient ligand-mediated TCR down-regulation. Journal of Immunology **168:** 4519-4523.
**Watanabe, E., Shimada, T., Kuroyanagi, M., Nishimura, M., and Hara-Nishimura, I.** (2002). Calcium-mediated association of a putative vacuolar sorting receptor PV72 with a propeptide of 2S albumin. Journal of Biological Chemistry **277:** 8708-8715.
**Watanabe, E., Shimada, T., Tamura, K., Matsushima, R., Koumoto, Y., Nishimura, M., and Hara-Nishimura, I.** (2004). An ER-localized form of PV72, a seed-specific vacuolar sorting receptor, interferes the transport of an NPIR-containing proteinase in Arabidopsis leaves. Plant & Cell Physiology **45:** 9-17.

## Figures

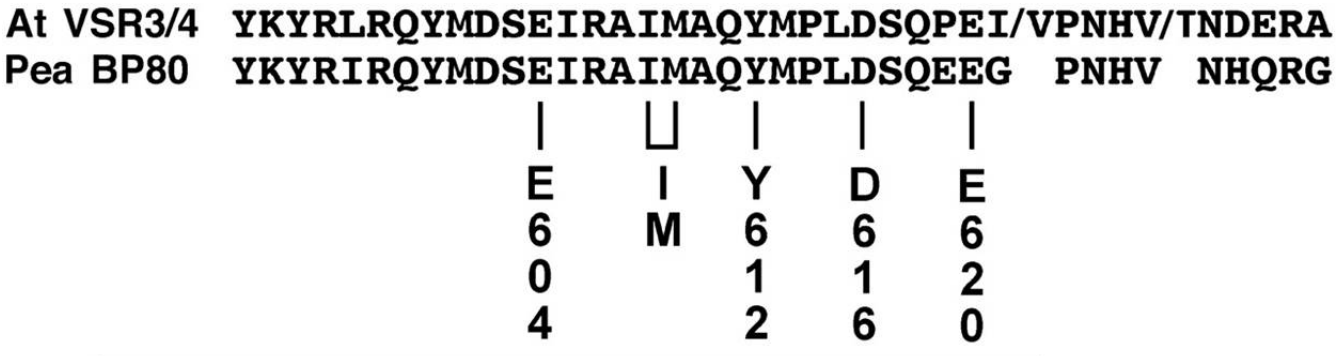


| | E604 | IM | Y612 | D616 | E620 |
|---|---|---|---|---|---|
| PS1 | | | | | |
| E604A | X | | | | |
| IMAA | | X | | | |
| Y612A | | | X | | |
| D616A | | | | X | |
| E620A | | | | | X |
| Y612A + E604A | X | | X | | |
| IMAA + Y612A | | X | X | | |
| Y612A + D616A | | | X | X | |
| Y612A + E620A | | | X | | X |

**Figure 1 :** Cytosolic sequence of BP80 and mutations used in this study.
The cytosolic sequence of pea BP80 and its closest Arabidopsis homologues AtVSR3 (At2g14740) and AtVSR4 (At2g14740) were aligned. A few amino acids were chosen based on their homology with mammalian signals and were mutated into alanine. The respective mutated cytosolic domains were fused together with the transmembrane sequence of BP80 to the reporter GFP to give raise to mutated reporter E604A, IMAA, Y612A, D616A and E620A. Position of the mutated amino-acids was numbered based on AtVSR3 sequence.

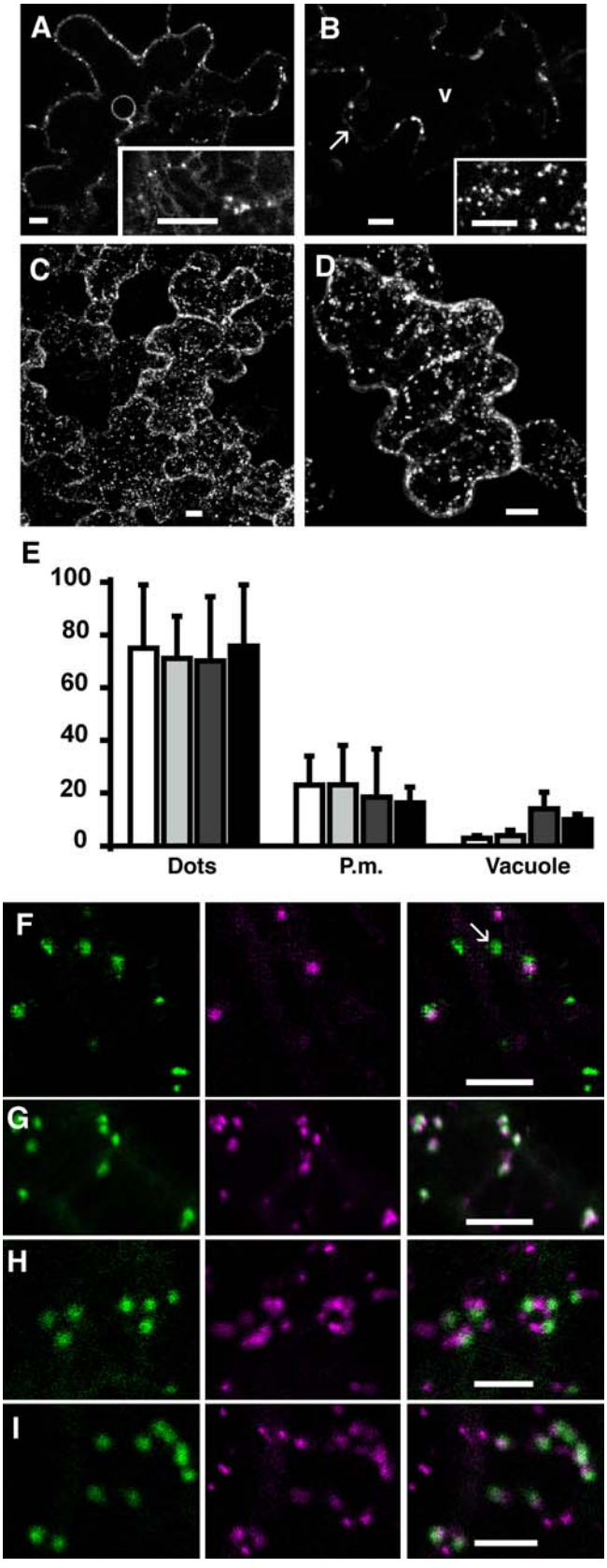
A
B
v
C
D
E
100
80
60
40
20
0
Dots
P.m.
Vacuole
F
G
H
I

**Figure 2** : Mutations of single acidic amino acids have minor effects on the localization of the reporter.
Tobacco epidermal cells transiently expressing reporter proteins were observed either 48h (A) or 72 hours (B to I) after transformation.
(A) The control reporter PS1, without mutation in the cytosolic sequence, was found in spots and ER at early stage of expression as seen in a section through the nucleus and in a section at the surface of the cell (inset). (B) After 72h of expression, the reporter has reached its final destination as seen in a section crossing through the vacuole (v) at the level of the nucleus with little labeling at the plasma membrane (arrow). Typical punctate structures can be better vizualized in an optical section through the cytosol (inset). (C) Accumulation of individual z sections of cells expressing PS1 reporter. (D) Accumulation of individual z sections from a cell expressing E604A mutated reporter. (E) Relative fluorescence intensity in three chosen locations, dots, plasma membrane (P.m.) and vacuole for the following constructs; control PS1 (white), E604A (light grey), D616A (dark grey) and E620A (black). (F to I) Tobacco epidermal cells transiently co-expressing PS1-based reporter proteins (green) and the Golgi reference ERD2-CFP (purple). The reporter protein was either PS1 (F), E604A (G), D616A (H) or E620A (I). (F) typical prevacuole labeling (arrow) is separated from Golgi labeling.
Scale bars, 10μm (A to D) or 5μm (F to I).

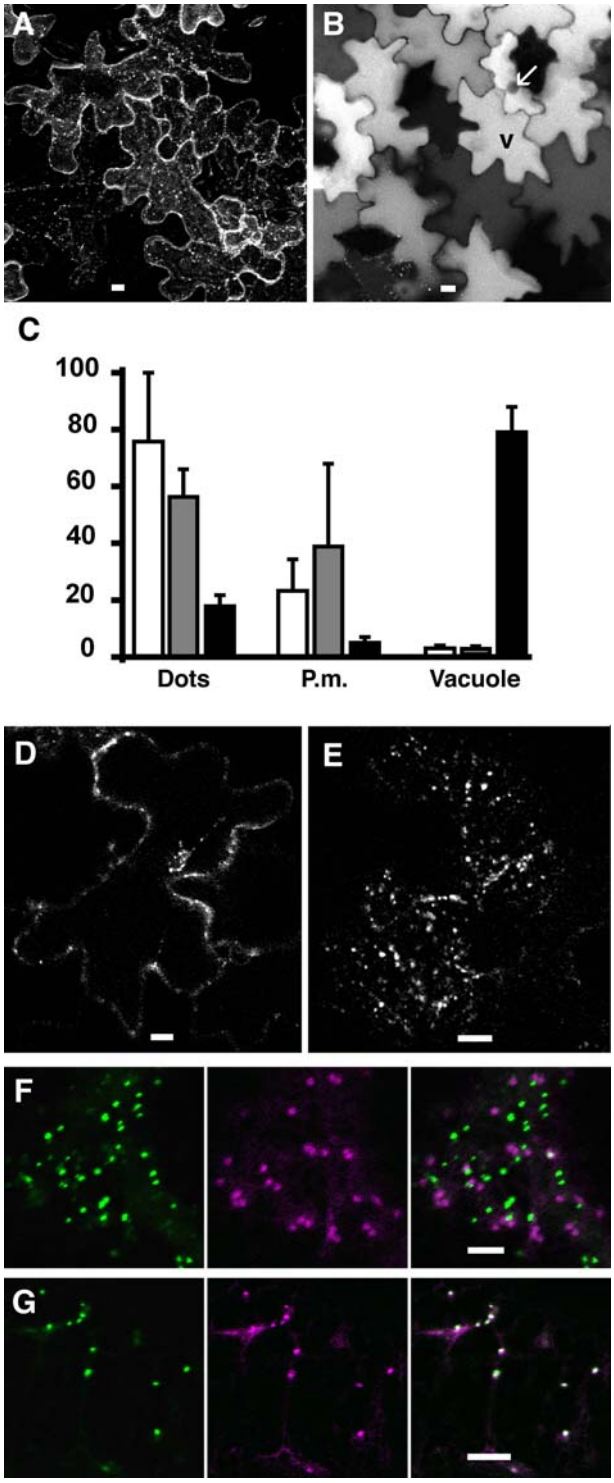


**Figure 3** : The Y612A mutation increases the presence of reporter at the plasma membrane while the IMAA mutation leads to GFP accumulation in the vacuole.
Tobacco epidermal cells transiently expressing reporter proteins were observed either 72h (A to C) or 48 hours (D to G) after transformation using a confocal microscope. (A) Accumulation of individual z sections from cells expressing Y612A. (B) A single section of cells expressing the IMAA reporter shows a massive fluorescence accumulation in the vacuole (v) leading to a

negative staining of the nucleus (arrow). (C) Relative fluorescence intensity in three chosen locations, dots, plasma membrane (P.m.) and vacuole for the following constructs; control PS1 (white), Y612A (grey) and IMAA (black). (D and E) Single sections at the level of the nucleus (D) or at the surface (E) for cells expressing IMAA show intermediate labeling of spots prior to vacuole accumulation. (F and G), coexpression of IMAA (green) either with a Golgi reference Erd2CFP (F, purple) or with the BP80 ligand Aleu-CFP (G, purple).
Scale bars, 10μm (A, B, D and E) or 5μm (F and G)

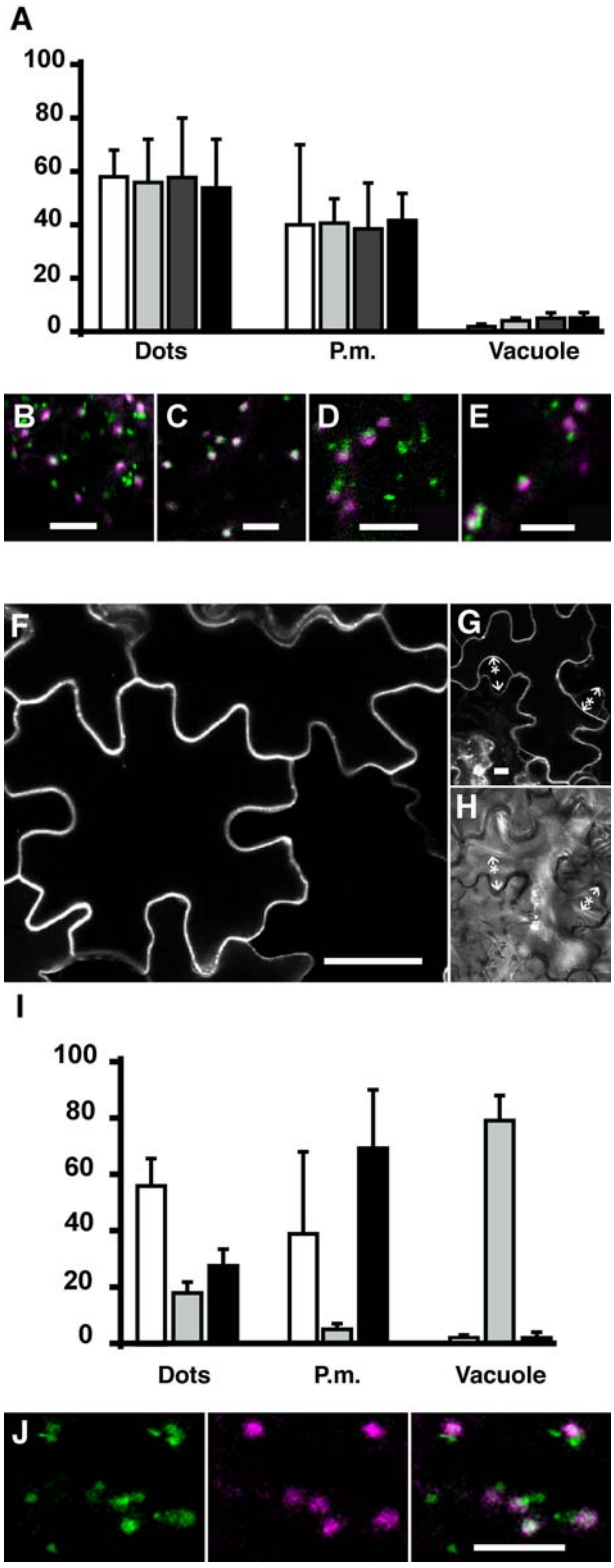


**Figure 4** : In the absence of a functional tyrosine motif, the IMAA mutation blocks the reporter in the plasma membrane while mutating acidic amino acids have minor effects.

Tobacco epidermal cells expressing transiently reporter proteins were observed 72h after transformation using a confocal microscope.
(A) Relative fluorescence intensity in three chosen locations, dots, plasma membrane (P.m.) and vacuole for the following constructs; Y612A (white), Y612A+E604A (light grey), Y612A+D616A (dark grey) and Y612A+E620A (black).. (B to E) Co-expression of the reporter proteins Y612A (B, green), Y612A+E604A (C, green), Y612A+D616A (D, green) or Y612A+E620A (E, green) with the Golgi reference ERD2-CFP (purple).
(F to H) Single confocal section of epidermal cells taken at the level of the nucleus, under normal condition (F) or after plasmolysis (G and H). (I) Relative fluorescence intensity in three chosen locations, dots, plasma membrane (P.m.) and vacuole for the following constructs; Y612A (white), IMAA (grey) and IMAA+Y612A (black). (J) Co-expression of IMAA+Y612A (green) with a Golgi reference ERD2-CFP (purple).
Arrow, cell wall. Arrow with a star, plasma membrane.
Scale bars, 5μm (B to E and J) or 10μm (F and G).

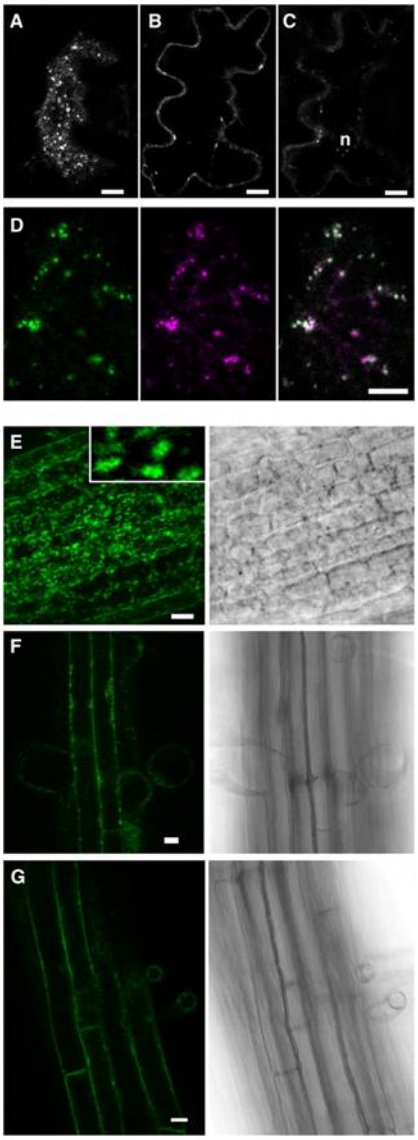

**Figure 5 :** A full length VSR fused to a fluorescent protein partially localizes in the plasma membrane and colocalizes with the PS1 reporter
(A to D) Tobacco epidermal cells transiently expressing reporter proteins were observed 72h after transformation using a confocal microscope.
(A to C) Confocal sections of an epidermal cell expressing citrine-AtVSR4 taken either at the surface (A), deeper inside the cell (B) or at the level of the nucleus (C).
(D) Co-expression of PS1 fused to CFP (green) with citrine-AtVSR4 (purple).
(E to G) Arabidopsis plantlets stably expressing citrine-AtVSR4. Roots from 7 days old plants were observed with a confocal microscope at different level, the apex (E), the middle portion (F) or the upper part (G).
n, nucleus. Scales bars 10µm

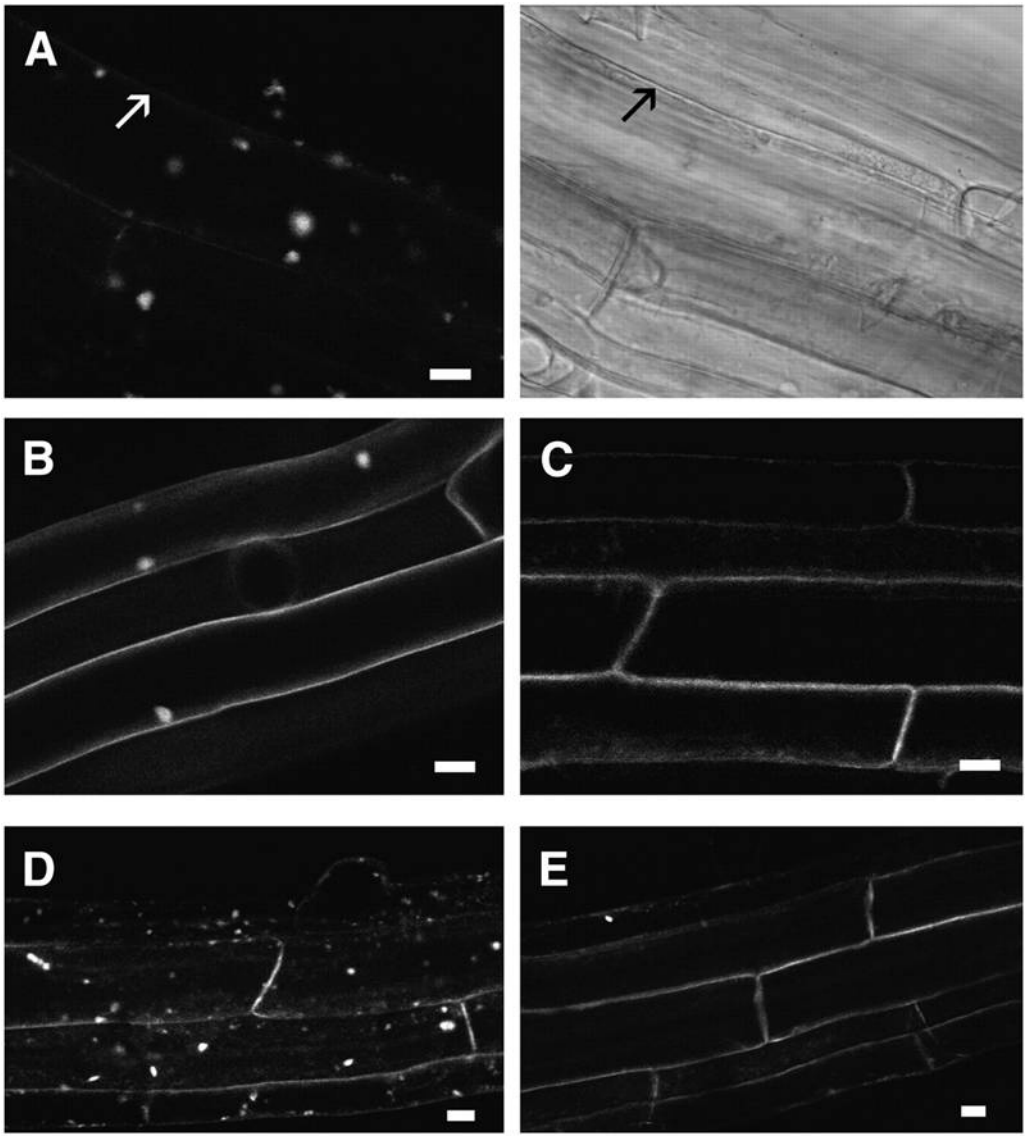


**Figure 6** : Citrine-AtVSR4 undergoes BFA sensitive endocytic recycling
One week old-plants expressing citrine-AtVSR4 were submitted to BFA treatment (50µM) for 60 minutes in presence of 50µM cycloheximide. Cells from the upper portion of the root, where the

fusion protein is exclusively found in the plasma membrane, were observed using a confocal microscope. (A) Citrine-AtVSR4 labeling after BFA treatment. (B) Control plants expressing LTi6a-GFP after BFA treatment. (C) Citrine-AtVSR4 after 60min cycloheximide treatment. Plasma membrane labeling of citrine-AtVSR4 had fully recovered after BFA treatment for 10min (D) and a subsequent wash in cycloheximide for 80min (E).

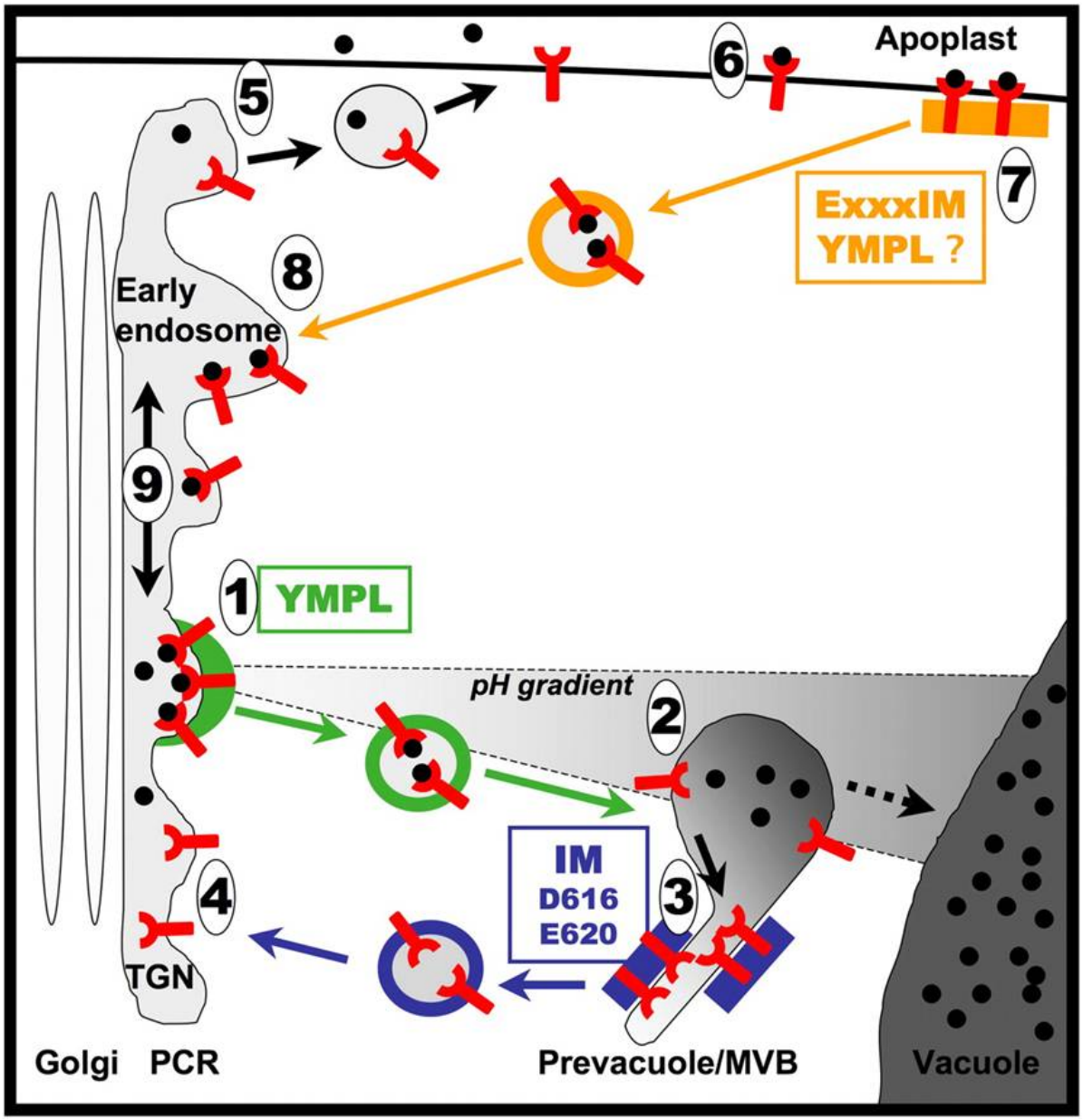


**Figure 7 :** Proposed trafficking model for the vacuolar sorting receptor BP80
The receptor BP80 uses a major (double arrows) or an alternative (arrows) pathway.
In the major pathway, BP80 recognizes the ligand (black circle) at the level of the *trans*-Golgi Network (TGN) that is part of a partially coated reticulum (PCR). The exit from the TGN (1) requires the YMPL motif most likely through its interaction with µA-adaptin containing complex (cross lines box and vesicle coat). After fusion of the vesicle to the prevacuole (2), due to a

possible pH decrease, the receptor releases its ligand. The free receptor is then segregated out of the ligand-release area (3) most likely by interaction of the IM motif with a retrieval complex (box and vesicle coat with vertical stripes) that remains in this compartment. The free receptor is packed in coated vesicles back to the TGN where fusion (4) may require VPS45. The final steps for ligand transport to the vacuole (5) do not require BP80 but instead are believed to be a maturation processes of the prevacuoles that eventually fuse with the vacuole.
The alternative pathway serves to retrieve misssorted ligands from the apoplast. The free receptor but also free ligand can exit the PCR (6) to reach the plasma membrane most likely as a default process. At the plasmalemma, the receptor binds a ligand (7) and is endocytosed using the IM dipeptide as part of a dileucine-like motif ExxxIM possibly with the help of the tyrosine motif. The endocytosis signal should interact (8) with the retrieval complex (box and vesicle coat with horizontal stripes). Fusion of the coated vesicle with the early endosome (9) leads to release the receptor-ligand complex in the PCR where the complex can diffuse along the membrane (10) and may enter the main pathway thanks to the tyrosine motif (1).

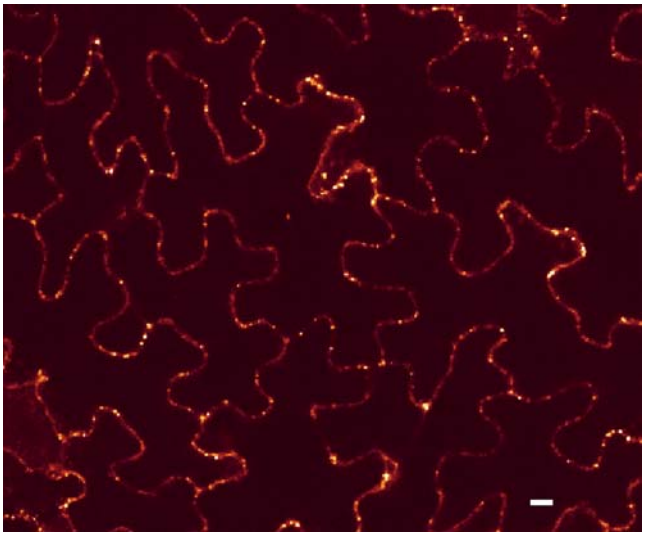

**Supplemental figure 1** : Expression of PS1 fusion protein in tobacco plants.
Stable transformant of tobacco expressing the fusion protein PS1 were grown and young leaves were observed with the confocal microscope.
Scale bar, 10µm

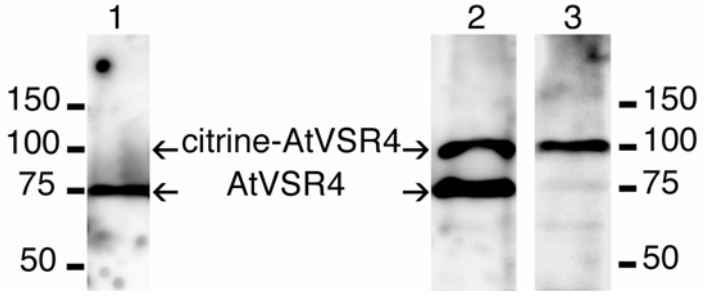

**Supplemental figure 2** : Arabidopsis expressing stably the construct citrine-AtVSR4 produce the fusion protein in a similar amount than the native homologue.
Immunoblot were performed on total proteins from wild type roots (lane 1) or roots expressing citrine-AtVSR4 (lanes 2 and 3). Affinity purified anti-AtVSR4 (lane 1 and 2) or anti-GFP antibodies (lane 3) were used. Positions for AtVSR4 (80kDa) and citrine-AtVSR4 (103kDa) are identified with arrows.

**Supplemental methods**

For immunolabeling analysis, plants were grown for 18 days as described previously (Kilian et al., 2007). More precisely seeds grown for 13 days on MS/2 plates and were transferred in liquid medium on floating rafts for 5 days in long-day conditions. Expression was checked under confocal microscopy prior to protein extraction. Tissue was rapidly frozen in liquid nitrogen and ground to a fine powder using a pilar and a mortar. Proteins were extracted 10 min at 60°C in 4% SDS, 65mM Tris-HCl pH 6,8. Large aggregates were removed by centrifugating at 13000 g for 10 min. The supernatant was adjusted to loading buffer for SDS-PAGE and boiled for 5 minutes (Laemmli, 1970). A quantity of 10µg to 20 µg of total protein was loaded, separated in a 12% SDS gel and transferred on nitrocellulose. As primary antibodies, we used affinity purified IgGs (1µg/ml) raised against a C-terminal peptide from AtVSR4 (PEVPNHTNDERA) and anti-GFP (Molecular probes A6455, 1/2000) to identify the fusion protein citrine-AtVSR4. Immunolabelled proteins were revealed using secondary antibodies coupled to horseradish peroxidase (Bio-Rad, 1721019) and chemiluminescence (Millipore P90720). Signal recovery and measurement was performed using a Fuji LAS-3000 system (exposure times from 10 sec to 30 sec).

**Kilian, J., Whitehead, D., Horak, J., Wanke, D., Weinl, S., Batistic, O., D'Angelo, C., Bornberg-Bauer, E., Kudla, J., and Harter, K. (2007). The AtGenExpress global stress expression data set: protocols, evaluation and model data analysis of UV-B light, drought and cold stress responses. The Plant Journal 50: 347-363.**
**Laemmli, U.K. (1970). Cleavage of structural proteins during the assembly of the head of bacteriophage T4. Nature 227: 680-685.**